NeuroImage: Clinical 11 (2016) 530–537

Contents lists available at ScienceDirect

NeuroImage: Clinical

journal homepage: www.elsevier.com/locate/ynicl

Autonomic correlations with MRI are abnormal in the brainstem vasomotor centre in Chronic Fatigue Syndrome

Leighton R. Barnden [a,b,*], Richard Kwiatek [c], Benjamin Crouch [a], Richard Burnet [d], Peter Del Fante [e]

[a] Department of Nuclear Medicine, The Queen Elizabeth Hospital, Woodville, SA 5011, Australia
[b] National Centre for NeuroImmunology and Emerging Diseases, Griffith University, Gold Coast, QLD 4222, Australia
[c] Division of Medical Subspecialities, Lyell McEwin Hospital, Elizabeth, SA 5112, Australia
[d] Endocrinology Department, Royal Adelaide Hospital, Adelaide, SA 5000, Australia
[e] Healthfirst Network, Woodville, SA 5011, Australia

ARTICLE INFO

Article history:
Received 21 November 2015
Received in revised form 21 March 2016
Accepted 23 March 2016
Available online 31 March 2016

Keywords:
Chronic fatigue syndrome
MRI
Autonomic
Regression
Vasomotor centre
Hypothalamus
Midbrain
Nerve conduction
Posture
Heart rate
Blood pressure
Anxiety and depression

ABSTRACT

Autonomic changes are often associated with the chronic fatigue syndrome (CFS), but their pathogenetic role is unclear and brain imaging investigations are lacking. The vasomotor centre and, through it, nuclei in the midbrain and hypothalamus play a key role in autonomic nervous system regulation of *steady state* blood pressure (BP) and heart rate (HR). In this exploratory cross-sectional study, BP and HR, as indicators of autonomic function, were correlated with volumetric and T1- and T2-weighted spin-echo (T1w and T2w) brain MRI in 25 CFS subjects and 25 normal controls (NC). Steady state BP (systolic, diastolic and pulse pressure) and HR in two postures were extracted from 24 h blood pressure monitoring. We performed (1) MRI versus autonomic score interaction-with-group regressions to detect locations where regression slopes differed in the CFS and NC groups (collectively indicating abnormality in CFS), and (2) MRI regressions in the CFS and NC groups alone to detect additional locations with abnormal correlations in CFS. Significant CFS regressions were repeated controlling for anxiety and depression (A&D). Abnormal regressions were detected in nuclei of the brainstem vasomotor centre, midbrain reticular formation and hypothalamus, but also in limbic nuclei involved in stress responses and in prefrontal white matter. Group comparisons of CFS and NC did not find MRI differences in these locations. We propose therefore that these regulatory nuclei are functioning correctly, but that two-way communication between them is impaired in CFS and this affects signalling to/from peripheral effectors/sensors, culminating in inverted or magnified correlations. This single explanation for the diverse abnormal correlations detected here consolidates the conclusion for a brainstem/midbrain nerve conduction deficit inferred earlier (Barnden et al., 2015). Strong correlations were also detected in isolated NC regressions.

1. Introduction

The chronic fatigue syndrome or myalgic encephalomyelitis (CFS) is a common, debilitating, multisystem disorder of uncertain pathogenesis, for which there exists evidence of dysregulation of the central nervous system, immune system and cellular energy metabolism (Carruthers et al., 2011). Dysregulation of the autonomic nervous system has also been suggested to contribute to its presentation (Gerrity et al., 2002; Van Cauwenbergh et al., 2014; Beaumont et al., 2012; Burton et al., 2010; Newton et al., 2007; Boneva et al., 2007; He et al., 2013).

The autonomic nervous system (ANS) contributes to the control of arterial pressure, heart rate and contractility, gastric and salivary excretions, blood vessel dilatation/constriction, temperature, immune and many other functions (Hall, 2011). It is conceptualised as descending from the hypothalamus via nuclei in the brainstem rostral medulla and caudal pons to peripheral target organs via the sympathetic nervous system (SNS) and parasympathetic nervous system (PNS) which also return sensory signals to the brain (Hall, 2011). The SNS and PNS both influence the enteric nervous system which controls gut activity (Hall, 2011).

Abbreviations: 1s, 1 sample; 2s, 2 sample; A&D, anxiety and depression; BA, Brodmann Area; BP, blood pressure; *ccP*, corrected cluster *P* statistic; Cb, cerebellum; CFS, chronic fatigue syndrome; CnF, cuneiform nucleus of the reticular formation; diaBP, diastolic blood pressure; DLPF, dorsolateral prefrontal; FDR, false discovery rate; FWE, family wise error; GM, grey matter; HADS, Hospital Anxiety and Depression Scale; HR, heart rate; NC, normal controls; PCC, posterior cingulate cortex; PHg, parahippocampal gyrus; POTS, postural orthostatic tachycardia syndrome; PP, pulse pressure; RAS, reticular activation system; SS, symptom score; sysBP, systolic Blood pressure; *uvP*, uncorrected voxel *P* statistic; VBIS, voxel based iterative sensitivity; WM, white matter.

* Corresponding author at: National Centre for NeuroImmunology and Emerging Diseases, Griffith University, Gold Coast, QLD 4222, Australia.
E-mail addresses: l.barnden@griffith.edu.au, siesta2@bigpond.com (L.R. Barnden), rkwiatek@bigpond.com (R. Kwiatek), benjamin.crouch@health.sa.gov.au (B. Crouch), hair77@bigpond.com (R. Burnet), peter.delfante@healthfirst.org.au (P. Del Fante).

http://dx.doi.org/10.1016/j.nicl.2016.03.017

In CFS an impaired ANS has been implicated in a variety of functional differences with healthy controls. Recent systematic reviews concluded that postural orthostatic tachycardia syndrome (POTS) is more prevalent and more severe in CFS, and (independent of the presence of POTS) heart rate is higher on head-up tilt testing (3). However, the prevalence of POTS in CFS was less than 30% (Van Cauwenbergh et al., 2014; Lewis et al., 2013). Baseline (supine) heart rate (HR) is elevated in some, but not all studies, and bedside autonomic tests are normal (Van Cauwenbergh et al., 2014). Heart rate variability (HRV), at least at night, is reduced in CFS (Meeus et al., 2013). A cardiac MRI study in CFS demonstrated substantially reduced left ventricular mass, end-diastolic volume and cardiac output, and increased residual torsion in diastole (Jones et al., 2012), which the authors suggest could be a consequence of the reduced total blood volume observed in CFS (Hurwitz et al., 2010).

Apart from the hemodynamic system, apparent autonomic deficits in CFS include delayed gastric emptying (Burnet and Chatterton, 2004), increased intestinal permeability (Maes et al., 2006) and impaired thermoregulation (Wyller et al., 2007; Pazderka-Robinson et al., 2004). Recently, a reduced capacity to recover from exercise-induced muscular acidosis in CFS was attributed to ANS-mediated dysfunction of Na^+–H^+ antiporters and/or vascular drainage (Jones et al., 2012; Jones et al., 2010).

Although neuroimaging has been used to identify the neural correlates of HR and/or BP response to various *stressors* (Beacher et al., 2009; Gianaros and Sheu, 2009; Critchley et al., 2000; Cechetto and Shoemaker, 2009), direct neuroimaging correlations with *steady state* autonomic levels *in healthy controls* are few. MRI studies of steady state BP in NC have mostly investigated GM volume associations, although in a meta-analysis (Beauchet et al., 2013) only two studies used a voxel-based method to investigate the whole brain for regional volume correlations, as is used here. Most studies of BP versus GM volume have examined hypertension, although one voxel-based study examined healthy elderly controls (Gianaros et al., 2006) and detected negative correlations, but only in men, in the supplementary motor area, anterior cingulate cortex and middle temporal gyrus. Importantly though, steady state muscle sympathetic nerve activity, a direct measure of the vasoconstrictor drive which mediates blood pressure, was found to correlate with fMRI BOLD signal in the medulla, hypothalamus and limbic nuclei (James et al., 2013; Macefield and Henderson, 2010). Despite autonomic dysfunction being accepted as evidence that CFS is a disorder of the central nervous system (Nijs and Ickmans, 2013), imaging studies of the neural correlates of autonomic function in CFS are also lacking.

Here we report extensive results from brain MRI regressions with autonomic function (as indirectly measured by steady state BP and HR in two postures), which reveal patterns of abnormality that provide new insights into brain-body relationships in CFS and are consistent with a nerve conduction deficit in the brainstem/midbrain.

In addition to grey matter (GM) and white matter (WM) volume images from voxel-based morphometry (VBM), we have utilised novel quantitative analysis of T1-weighted (T1w) and T2-weighted (T2w) spin-echo brain MRI images, after inter-subject signal-level normalisation (Abbott et al., 2009). T1w and T2w spin-echo images are ideal for cross-sectional studies because of their low-noise, high resolution and minimal distortion from the patient-induced and instrumentation-induced magnetic field inhomogeneities (Bushberg et al., 2002) that distort gradient-echo scans.

Control of steady state BP and HR involves the vasomotor centre in the rostral medulla and lower third of the pons. In turn, the hypothalamus and reticular substance of the pons, midbrain and diencephalon can excite or inhibit the vasomotor centre, and to some extent the autonomic centres in the brainstem medulla act as relay stations for control activities of the hypothalamus and midbrain (Hall, 2011). Our hypothesis was that in CFS these locations may exhibit abnormal brain MRI correlations with the autonomically controlled peripheral BP and HR scores assessed here and, for statistical purposes, they were assigned *a priori* hypothesis status.

2. Materials and methods

25, otherwise well, CFS subjects from community-based specialist and general practice, meeting Canadian Consensus criteria (Carruthers et al., 2011) for CFS, with a mean duration of fatigue of 7.4 years (range, 2–15 years) were assessed. 25 healthy, normal controls (NC), unrelated to the CFS subjects, recruited by public advertisement, and matched for gender, age to within 2 years and weight to within 5 kg were also recruited. Each group comprised six men and 19 women. The mean ages were 32 years (range, 19–46 years) for CFS subjects and 32.8 years (range, 20–46 years) for NCs. The precursor to CFS onset was an infection in 14 cases (seven caused by serologically proven Epstein–Barr virus), work and stress in three, post-delivery in one and was unknown in seven. On clinical grounds, none had POTS (Schondorf and Low, 1993). All medications including 'natural therapies' were discontinued 2 weeks before the study period, except for paracetamol and oral contraceptives. No subjects had been taking vasoactive drugs. Subjects with a body mass index >30 kg/m^2, or who were pregnant, postmenopausal, unable to undertake brain MRI, or unable to discontinue medication were excluded. The study period was delayed for any viral or bacterial infection until recovery. All examinations were completed within a week. All participants completed the Hospital Anxiety and Depression Scale (HADS) (Zigmond and Snaith, 1983) questionnaire.

This work was carried out in accordance with *The Code of Ethics of the World Medical Association (Declaration of Helsinki) for experiments involving humans.*

2.1. BP and HR monitoring

Autonomic status was assessed with 24-hour ambulatory blood pressure monitoring (ABPM) which, every 30 min between 7 a.m. and 10 p.m. and hourly between 10 p.m. and 7 a.m., recorded values for systolic BP (sysBP), diastolic BP (diaBP), pulse pressure (PP = sysBP–diaBP) and heart rate (HR), collectively referred to here as hemodynamic scores. To segregate postural effects, ABPM values were extracted for periods when the subjects were lying down asleep, labelled hereafter as *reclining*, and when they were seated awake with torso upright, labelled hereafter as *erect*. These periods were identified from a diary of posture (standing, seated, lying down awake or lying down asleep) for each measurement time, updated by each participant at least every 2–3 h or on awakening. For each measure, the mean of all recorded erect values and the mean of all reclining values for each subject were computed. In a preliminary report (Barnden et al., 2011) these postures were called *asleep* and *seated* respectively. Two NC subjects did not have ABPM data and were excluded from regressions. A third NC did not record any seated period and was excluded from the erect posture regressions.

2.2. MRI acquisition

Magnetic Resonance images were acquired on a Philips 1.5T Intera MR scanner (Philips, Eindhoven) with a body transmit coil and birdcage receive coil. Three sequences were used: T1-weighted spin echo (T1w, TR/TE/flip angle = 600 ms/15 ms/90°), T2-weighted spin-echo (T2w, 4000/80/90°) and 3D spoiled gradient echo (5.76/1.9/9°). T1w and T2w images were transaxial with pixel sizes 0.82 × 0.82 mm and 0.859 × 0.859 mm respectively and 3 mm contiguous slice thickness. The 3D gradient echo voxel size was 0.938 × 0.938 × 1.0 mm.

2.3. Preprocessing of images

Four MRI image types were analysed: Grey matter (GM) volume and white matter (WM) volume from voxel-based morphometry (VBM), and T1-weighted and T2-weighted spin-echo (T1w and T2w). Image processing is described fully in (Barnden et al., 2015).

T1w and T2w signal levels were normalised using the voxel-based iterative sensitivity (VBIS) method of Abbott et al (Abbott et al., 2009). VBIS requires an initial CFS group comparison with NC using T1w (or T2w) images scaled using their global means ('proportional scaling'). A mask is then defined containing those voxels with residual inter-subject variance less than the median. The mean in this mask is then computed for each image and used as a nuisance covariate in subsequent statistical designs, effectively normalising each image to a common global value. To exclude possible bias in individual analyses, a second iteration of VBIS omitted voxels from this mask where a signal with uncorrected voxel $P < 0.01$ was detected. Here we applied the second iteration to the two designs which yielded the largest clusters, for which VBIS would be most sensitive to any incidental bias-inducing signal within the mask.

2.4. Statistical analysis

Cluster statistical inference in SPM5 (http://www.fil.ion.ucl.ac.uk/spm) was used to identify brain locations where MRI versus hemodynamic score regressions were significant. Four statistical designs were systematically applied to the datasets of all 4 types of MR image:

A. MRI regressions against hemodynamic scores to identify voxels where the CFS and NC regressions exhibited opposite slopes. These so-called interaction-with-group (2-sample or '2s') regressions detected brain locations where the CFS relationship was explicitly abnormal.
B. MRI regressions against hemodynamic scores in the CFS group alone (1-sample or '1s'). The corresponding 2-sample regression would *not* detect a significant cluster *if*:

- The local NC inter-subject variance was large, so that neither the NC regression nor the difference between the NC and CFS regression slopes could be significant. A significant CFS regression in this case is of interest and may be regarded as abnormal.
- The NC regression was *significant* and with a similar slope to the CFS regression. If they yielded co-located significant clusters, the CFS relationship did not differ from NC and was not considered relevant to CFS. Note that 1s regressions were not considered in the preliminary report (Barnden et al., 2011).

C. MRI regressions against hemodynamic scores in the NC group alone, but only for regressions from (A) and (B) that yielded significant clusters.
D. MRI group comparisons for GM volume, WM volume, T1w and T2w images.

All regressions were adjusted for age. Initially, clusters were formed with an uncorrected voxel P (*uvP*) of 0.005 and regressions that yielded clusters with *corrected* cluster $P < 0.05$ were then repeated adjusting (controlling) for Anxiety and Depression (A&D). For a priori locations, adjustment was also performed for clusters with *uncorrected* cluster $P < 0.05$. This was only invoked, however, if the *corrected* cluster P failed to survive the final False Discovery Rate (FDR) threshold (see below). Finally, only clusters formed with $uvP < 0.001$, either before or after adjustment for A&D, were reported, but only if they survived the multiple comparisons constraint below.

2.5. Adjustment for multiple regressions

Two corrections of cluster statistics for multiple comparisons were performed (Barnden et al., 2015).

Firstly, correction within SPM5 was made for multiple clusters across space from each regression using the non-stationary permutation method (Hayasaka et al., 2004).

Secondly, to account for multiple regressions, a FDR < 0.05 constraint was applied. A total of 200 regressions were performed (Barnden et al., 2015). Of these, $4 \times 2 \times 16 = 128$ involved the autonomic regressors considered here. '4' represents the four MR image types (GM volume, WM volume, T1w and T2w), '× 2' accounts for positive and negative regressions and '× 16' represents the four ABPM regressors (sysBP, diaBP, PP and HR) each in two postures and each analysed with 2 statistical designs (A and B above). Note that 200 (not 128) was used in the FDR analysis to identify a cluster P threshold consistent with FDR < 0.05 (see Barnden et al., 2015). Also of interest were clusters that survived

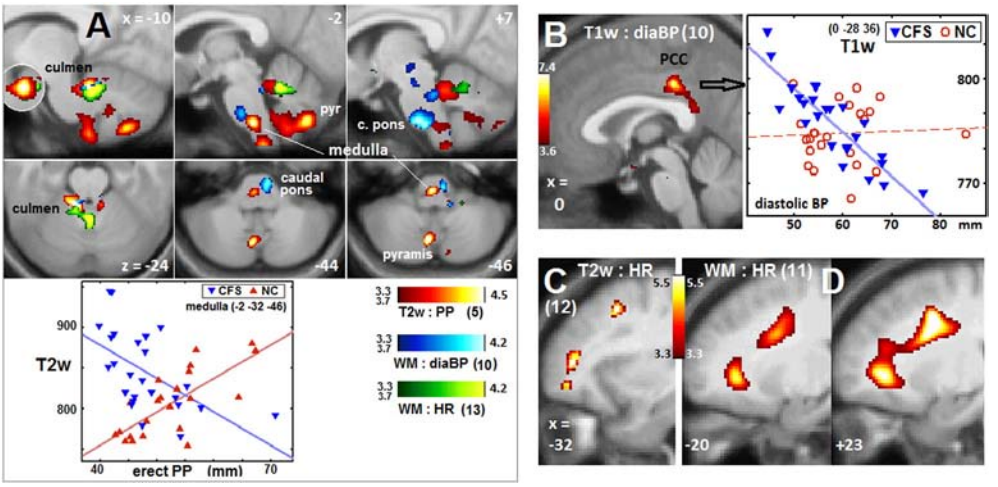

Fig. 1. Brainstem vasomotor centre, cerebellum, PCC and prefrontal WM clusters. Sections through 8 clusters from Table 2. Coloured voxels code for the T statistic (refer colour stripes). Image type, basic hemodynamic score and (Table 2 cluster number) are annotated. The voxel P threshold for colour display was 0.001, except for 0.00025 (T = 3.7) for the lower (axial) panel of (A). Plots show T2w and T1w values for individual CFS and NC subjects (adjusted for age and global value) at the most significant voxels. Lines show the general linear model fits. (A) shows involvement of the rostral ventral medulla ($x = -2$), right caudal basal pons ($x = +7$), and culmen ($x = -10$) and pyramis ($x = -10$, -2 and $z = -44$, -46) of the cerebellar vermis. The $x = -10$ insert reverses the overlap at the culmen. (B) posterior cingulate cortex (PCC). For the CFS regression plotted, corrected voxel $P = 0.04$. (C) left prefrontal WM, and (D) left and right prefrontal WM.

the stricter Bonferroni *P* threshold, that is 0.05/200 = 2.5e-4, which is relevant if all regressors are uncorrelated.

If the *peak voxel* in a cluster had FWE-corrected *voxel P* < 0.05, this was also reported.

2.6. Identification of cluster locations

Cluster locations were refined using the TD and 'aal' databases incorporated in the WFU PickAtlas toolbox of SPM5, Duvernoy's brainstem atlas (Naidich et al., 2009) supported by MNI coordinates of its sections from (Lee et al., 2008), a hypothalamus atlas (Baroncini et al., 2012) and a whole brain atlas (Nolte and Angevine, 2000). All images are displayed using the 'neurological' convention (subject's left is left on the image) and the default *uvP* threshold of the clusters shown was 0.001. To better locate peaks within the clusters, clusters with a stricter *uvP* threshold are also included in Figs. 1 and 2.

3. Results

Here we report the neurocorrelates of *steady state* BP and HR from a wider exploratory MRI study conducted to seek insights into the etiology of CFS (Barnden et al., 2011, 2015). Because this is the first such study of BP and HR in CFS, a comprehensive set of hemodynamic regressors was investigated.

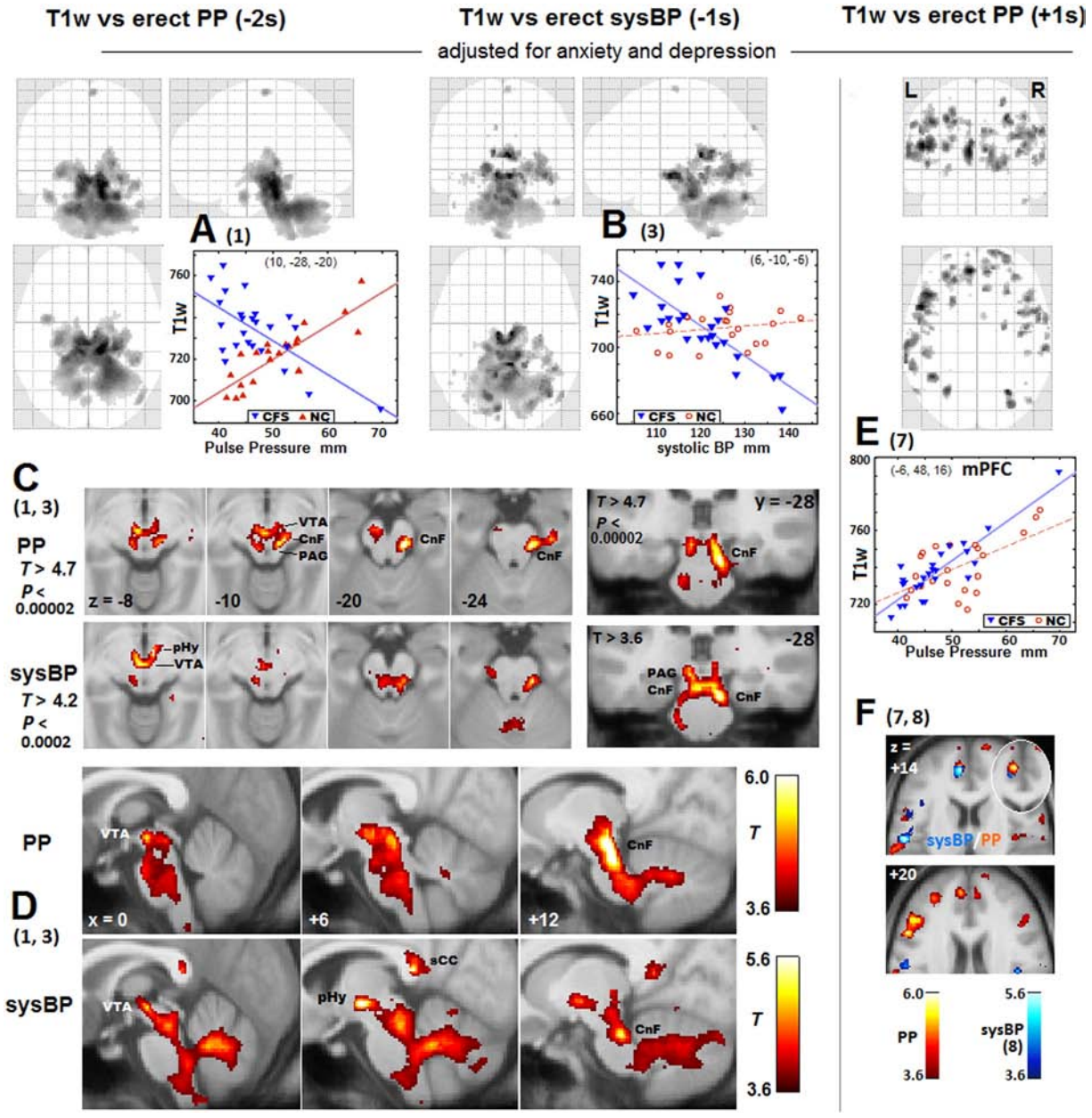

Fig. 2. Clusters from T1w regressions with erect PP and erect sysBP. Numbers (in parentheses) reference Table 2 regressions. Greyscale (upper panels) or colour (lower panels) levels represent the *T* statistic. The voxel *P* threshold for voxel display is 0.001 except as labelled in (C). In (A), (B) and (E) maximum T statistic projections show the spatial extent of the correlations. The two negative regressions yielded clusters of similar extent but with different peak locations. Beneath are transaxial (C and F), coronal (C) and sagittal (D) sections through peak voxels. A stricter threshold is applied in(C). In PP, this isolates two peaks in the reticular formation cuneiform nucleus (CnF) at z = −10 and −20 and one in the ventral tegmental area (VTA) at z = −10. In sysBP, there is posterior hypothalamus (pHy) peak adjacent to a VTA peak at z = −8. Sections in (F) show *positive* PP and sysBP regression clusters: at z = +14 in the medial prefrontal cortex for both (the elliptical insert reverses the overlap) and in the left postcentral somatosensory gyrus for sysBP; and at z = +20 in the left DLPF cortex for PP. In the 1s plots in (B) and (E), NC values, although not used in the analysis, are also shown (in red). The plot in (E) illustrates a case when the 1s NC analysis detected a co-located cluster and the CFS result was not regarded as abnormal.

3.1. HR, BP, anxiety and depression scores

A comparison between CFS and NC of all hemodynamic measures showed heart rate was significantly elevated in CFS for both erect and reclining postures and pulse pressure was reduced for the erect posture – see preliminary report (Barnden et al., 2011). HADS scores (mean ± SD) were, for depression, 8.4 ± 4.7 for CFS and 4.0 ± 3.3 for NC ($P < 0.0002$), and for anxiety, 6.6 ± 3.0 for CFS and 1.7 ± 2.3 for NC ($P < 0.0001$).

Table 1 lists Pearson correlations within the CFS group between pairs of the 8 hemodynamic scores and anxiety and depression (column 2). diaBP and sysBP correlated strongly for each posture (strongest reclining), though not as strongly between postures. For the same posture, PP correlated strongly with sysBP, but not diaBP. HR measures from the two postures were not correlated and neither correlated with any BP measure. Anxiety and Depression were strongly correlated ($P = 0.0001$) and both correlated negatively with erect PP. None of the 10 scores in Table 1 correlated with CFS duration. More correlations may be found in the supplementary data of the preliminary report (Barnden et al., 2011).

3.2. MRI correlations with BP and HR

3.2.1. General overview

For the 128 regressions surveyed with designs A and B, a false discovery rate of 0.05 was achieved for a cluster $P < 0.008$. 13/128 regressions (Table 2) yielded significant clusters. Eight of the 13 regressions were 2-sample (CFS and NC had opposite regression slopes) and five were 1-sample (CFS-only) regressions. Of the 4 MRI image types, T1w regressions yielded most clusters, but WM volume and T2w also contributed. All regressors (sysBP, diaBP, PP and HR) and both postures were involved.

Adjustment for anxiety and depression (A&D) was performed to address a concern that some changes in BP and HR in CFS may be a consequence of A&D. Before adjustment, 14 of the 19 clusters in Table 2 were significant (FDR < 0.05 via *ccP* < 0.008). Adjusting for A&D rendered another five significant, but 4 then became insignificant (bracketed *ccP adj*).

In one case, the same 1s regression in NC as for CFS, generated a co-located cluster (7 in Table 2, plot in Fig. 2E) and was discounted as relevant to CFS.

Plots in the Figures show values for individual subjects at the most significant voxel for 5 clusters. 1s plots also show NC values (circles) to illustrate why corresponding 2s regressions were insignificant at that voxel.

3.2.2. Bias from VBIS scaling of T1w and T2w?

VBIS (Abbott et al., 2009) was used here to estimate global levels to normalise T1w and T2w scans. To check for possible bias introduced by the VBIS mask that might have contributed to the correlations detected, we performed a second iteration of VBIS for vulnerable (large cluster) regressions (1 and 2 in Table 2). This omitted areas in the mask where the regression was significant. Voxels in the cluster formed with a relaxed voxel threshold (0.01) were omitted. This reduced the size of the T1w and T2w VBIS masks by 12% and 19%, respectively. With the new global values, however, the resulting cluster statistical inference was little changed. For regression 1, *ccP adj* remained at 2.5e-6, its size changed from 10510 to 10790 voxels, and the FWE-corrected *P* of the peak voxel changed from 0.0069 to 0.0074. For regression 2, *ccP adj* remained at 6.5e-6 and its size changed from 16589 to 16341 voxels. Therefore, bias was negligible and for all T1w and T2w designs here, global levels from the mask from a single iteration of VBIS were used.

Because vasomotor centre nuclei communicate directly with the peripheral effectors/sensors that determine the BP and HR used here as regressors, and vasomotor centre activity is modulated by midbrain and hypothalamus nuclei, we have ordered the location-specific results accordingly:

3.2.3. MRI correlations in the brainstem vasomotor centre

Fig. 1A shows sections through 6 clusters in the rostral medulla and caudal pons (vasomotor centre) and cerebellar culmen from 3 different regressions (Table 2 regressions 5, 10 and 13). This supports the hypothesis for an abnormal relationship between BP and HR and the vasomotor centre in CFS. The plot demonstrates the oppositely signed regressions for CFS and NC in the rostral medulla (cluster 5.2). The diaBP correlation (regression 10) in the caudal pons is consistent with its role in initiating *inhibitory* signals to decrease HR and contractility (Hall, 2011). When an isolated -1s NC regression corresponding to regression 10 was performed it detected a very significant cluster (*ccP* = 8e-5) co-located with the 2s cluster in the caudal pons.

3.2.4. MRI correlations in the midbrain

Fig. 2A, B illustrates the extended nature of clusters in the midbrain and hindbrain from T1w regressions with -PP and -sysBP (1,3 in Table 2). In Fig. 2C, stringent voxel thresholds locate isolated cluster peaks in the cuneiform nucleus of the reticular formation (CnF), ventral tegmental area (VTA), and posterior hypothalamus (sysBP only). For PP, the VTA and two CnF peaks were significant at the voxel level (FWE corrected voxel $P = 0.007, 0.01, 0.04$). The strength of the VTA peak for both PP and sysBP was much enhanced by adjusting for A&D.

Of note, the rostral medulla, lateral midbrain reticular formation (CnF) and posterior hypothalamus send *excitatory* signals to the heart (Hall, 2011) which is consistent with their correlations here with sysBP and, to a lesser extent, PP.

3.2.5. MRI correlations in the hypothalamus

The hypothalamus plays a key role in the control of BP and HR at rest and in stress (Hall, 2011). Four clusters were detected in nuclei of the hypothalamus. Two did not survive adjustment for A&D, however, and for two it was necessary to invoke the *a priori* status of the

Table 1
Correlations in CFS between hemodynamic scores and anxiety and depression. The R statistic is above and the *P* statistic below the diagonal. Only *P* values ≤0.05 (R ≥ 0.4) are shown. Numbers in the top row correspond to the numbered scores in columns 1.
HR: heart rate, sysBP: systolic blood pressure, diaBP: diastolic blood pressure, PP: pulse pressure.

		1	2	3	4	5	6	7	8	9	10
1	HR erect	x	0.35	−0.26	0.06	−0.13	0.14	0.09	0.15	−0.16	−0.14
2	HR reclining	.	x	−0.17	−0.08	0.02	0.09	0.20	0.22	0.01	−0.13
3	PP erect	.	.	x	0.43	0.67	0.21	−0.12	−0.07	−0.41	−0.45
4	PP reclining	.	.	0.032	x	0.39	0.79	0.08	0.31	−0.37	0.05
5	sysBP erect	.	.	0.0002	.	x	0.56	0.66	0.51	−0.20	−0.15
6	sysBP reclining	.	.	.	3e-6	0.003	x	0.54	0.83	−0.22	0.18
7	diaBP erect	.	.	.	.	0.0004	0.005	x	0.76	0.14	0.26
8	diaBP reclining	.	.	.	.	0.009	4e-7	1e-5	x	−0.01	0.24
9	anxiety	.	.	0.042	.	.	.	.	.	x	0.69
10	depression	.	.	0.024	.	.	.	.	.	0.0001	x

hypothalamus (i.e. consider *ucP*). Three are shown in Fig. 3. The posterior hypothalamus was correlated with the more challenging erect posture, while the anterior correlated with reclining posture measures.

3.2.6. MRI correlations in limbic areas

Some limbic nuclei affect BP and HR in response to stress. A reclining diaBP correlation was detected in the posterior cingulate cortex (PCC, Table 2 cluster 9, Fig. 1B) in CFS but not in NC. The PCC is a key nucleus of the default mode network which is active during rest/sleep. This is consistent with its correlation here with *reclining* (and asleep) diaBP.

3.2.7. MRI correlations in WM tracts

Regressions 11 and 12 with HR yielded clusters in prefrontal WM (Fig. 1C, D), and clusters 2 and 3 extended into the WM of the inferior fronto occipital fasciculus (IFOF). The isolated -1s NC regression corresponding to regression 11 detected a very significant cluster ($ccP = 7e\text{-}5$) co-located with the 2s cluster in right dorsolateral prefrontal WM.

3.2.8. MRI group differences

Simple MRI comparisons between CFS and NC groups (design D in Methods) only detected a significant cluster for T2w. This was in the supplementary motor area (−12, −22, 70) for CFS > NC (A&D adjusted $ccP = 0.0005$). A T2w cluster for CFS < NC was reported in middle temporal WM but for more relaxed statistical criteria (Barnden et al., 2015).

4. Discussion

This exploratory cross-sectional brain MRI study in CFS of correlations with peripheral BP and HR measures indicative of *steady state* autonomic nervous system function, is our third paper to analyse this common data set. All utilise cluster statistical inference from voxel-based analysis. The first (Barnden et al., 2011) was a preliminary report and the second (Barnden et al., 2015) a study of MRI associations with CFS severity and duration in white matter, which suggested a severity-dependent upregulation of prefrontal myelin which was interpreted as a plastic response to impaired brainstem/midbrain nerve conduction. This work examines MRI regressions with the autonomically controlled measures *steady state* BP and HR and, in common with the previous reports, is distinguished by some novel features:

- For the first time in CFS, quantitative analysis was performed with T1- and T2-weighted spin-echo images. Inter-subject signal levels were normalised with the VBIS method (Abbott et al., 2009). We also analysed grey and white matter volume images from VBM.
- We performed (1) MRI versus autonomic score interaction-with-group regressions which, at each voxel, test the CFS and NC regressions for opposite slopes, and (2) regressions in the CFS group alone. The first identifies locations where the collective CFS relationship is explicitly abnormal. Locations identified with the second were also regarded as having an abnormal relationship when the same 1s regression in the NC did not detect a co-located cluster.
- We repeated regressions to adjust for associations with anxiety and depression (A&D).

Interaction-with-group (2s) regressions are a very powerful tool here because they clearly demonstrate abnormal MRI correlations in CFS. It should be noted that abnormality only applies in a collective, population-wide sense. Two abnormal correlations in the vasomotor centre are particularly pertinent because nuclei in this area communicate directly via sympathetic and parasympathetic signalling with peripheral BP and HR effectors/sensors. Abnormal correlations were also detected in nuclei in the midbrain reticular substance and the hypothalamus which participate in the regulation of steady state BP and HR via reciprocal signalling with the vasomotor centre.

Table 2
Clusters from MR versus Hemodynamic Score regressions.
Details of 19 clusters, defined using voxel *P* threshold = 0.001, from 13 regressions ordered by 'Systolic BP or Pulse Pressure', 'Diastolic BP' and 'Heart Rate'. Their False Discovery Rates were <0.05 (cluster $P < 0.008$). Column 1 identifies both regression and cluster (n.2, n.3 for second, third cluster). cc*P* is corrected cluster *P* (corrected for multiple clusters). '*ccP adj*' is *ccP* after the regression was adjusted (controlled) for anxiety and depression. 'design' shows the sign of the CFS regression (− or +) and whether it was 2 sample (CFS and NC regressions with opposite-sign slopes), or 1 sample (CFS only). +1s/−1s means a positive/negative regression slope. +2s means (for HR say) a positive slope for CFS vs HR and a negative slope for NC vs HR, and vice versa for −2s. Where regression details are blank, refer to line above. 'ccP adj' entries in (parentheses) did not meet statistical criteria ($ccP < 0.008$), or there was a co-located cluster from the same-sign NC regression [square brackets].
BA Brodman Area, Cb cerebellum, CnF cuneiform reticular nucleus, diaBP diastolic blood pressure, DLPF dorsolateral prefrontal, HR heart rate, IFOF inferior fronto occipital fasciculus, LGP lateral globus pallidus, pHg parahippocampal gyrus, sysBP systolic blood pressure, PP pulse pressure, VTA ventral tegmental area, WM white matter.

Regression		Regression details					Corrected cluster *P*			Size (voxels)	
Cluster	Fig	MRI	Posture	Regressor	Design	Structure	x,y,z of peak	cc*P*	cc*P* adj		adj
Systolic BP or Pulse Pressure											
1	2A,C,D	T1w	erect	PP	−2s	[a]CnF, [a]VTA, pHg, LGP, hindbrain	10, −28, −20	4.7e-6	[a]2.5e-6	2939	10510
2		T1w	erect	PP	−1s	[a]CnF, [a]Cb, brainstem, pHg, LGP, IFOF	8, −26, −6	6.5e-6	[a]6.5e-6	10510	16589
3	2, 3	T1w	erect	sysBP	−1s	Posterior hypothalamus, VTA, CnF, Cb	6, −10, −6	1.3e-5	1.3e-5	4472	6497
3.2	2 A,D					Splenium of corpus callosum	6, −38, 12	ns	0.0007		218
3.3						R middle temporal WM (IFOF)	40, −66, −6	ns	0.0013		893
4		T1w	erect	sysBP	−2s	VTA	−4, −14, −2	ns	0.005		250
5	1A	T2w	erect	PP	−2s	Culmen of Cb vermis	−10, −42, −24	ns	0.003		689
5.2	1A					Rostral medulla	−2, −32, −46	ns	0.005		561
6	3	T1w	reclining	sysBP	−2s	[b]hypothalamus	6, 2, −18	[b]0.005	([b]0.02)	94	59
7	2E,F	T1w	erect	PP	+1s	[a]L medial prefrontal cortex	−6, 48, 16	[a]0.0003	[0.0009]	493	301
7.2	2E					L BA46, DLPF cortex	−50, 16, 22	0.001	0.0007	220	330
8	2E	T1w	erect	sysBP	+1s	L postcentral somatosensory	−54, −10, 16	0.0003	(0.01)	381	148
Diastolic BP											
9	1B	T1w	reclining	diaBP	−1s	[a]Posterior Cingulate Cortex	0, −28, 36	[a]0.001	[a]0.002	274	252
10	1A	white	erect	diaBP	+2s	caudal basilar pons, Cb culmen	7,−26,−44	0.003	0.002	975	1065
Heart Rate											
11	1D	White	Reclining	HR	−2s	[a]R prefrontal WM	26, 8, 27	[a]1.2e-5	[a]5.7e-6	3210	3380
11.2	1D					L prefrontal WM	−18, 8, 27	0.003	0.0009	1148	1228
12	1C	T2w	Erect	HR	−2s	L lateral prefrontal WM	−32, 46, 8	0.006	(0.01)	169	139
13	1A,3	White	Reclining	HR	+2s	[b]Culmen of Cb vermis	0, −51, −23	[b]0.0005	[b]0.002	790	660
13.2	3					[b]Hypothalamus	−5, −4, 12	[b]0.001	([b]0.02)	174	82

[a] Voxel peak(s) with FWE corrected $P < 0.05$.
[b] A priori location; uncorrected cluster P.

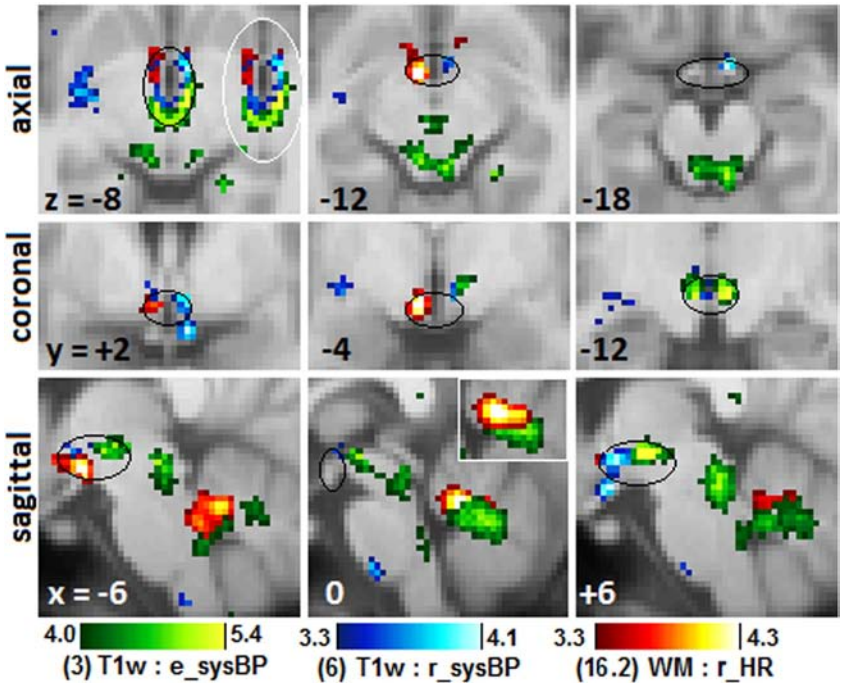

Fig. 3. Clusters in the hypothalamus. Magnified sections of clusters that show peaks of significance in the hypothalamus from 3 different MR regressions with erect and reclining systolic BP, and reclining HR (Table 2, clusters 3, 6, 16.2). Black ellipses loosely outline the hypothalamus. White-bordered inserts at $z = -8$ and $x = 0$ reverse the order of cluster overlap. There was little overlap at $z = -8$. Clusters were from regressions not adjusted for anxiety and depression. Sagittal sections also show clusters in the midbrain, brainstem and cerebellar vermis. In the hypothalamus, peaks were located in the posterior (green, blue), lateral (red) and anterior (red, blue) divisions. The green sysBP posterior hypothalamus cluster at $x = +6$ and $z = -8$ is also seen in Fig. 2(D) at $x = +6$.

Importantly, CFS versus NC group comparisons did not find differences in any of the nuclei with abnormal hemodynamic correlations. Thus, only when autonomic variables are included in correlational analysis does one find a relationship in CFS that differs from controls. It is possible therefore that the regulatory nuclei themselves may be unaffected, but that two-way signalling between them is compromised and this affects signals to/from peripheral autonomic effectors/sensors which culminates in the collective dysregulation in CFS expressed by the abnormal correlations here. This is consistent with the impaired midbrain nerve conduction in CFS inferred earlier (Barnden et al., 2015).

The NC correlation associated with a significant 2s cluster will not necessarily yield a significant cluster from an isolated (1s) NC analysis. When however, for each significant 2s regression, we performed a separate 1s regression in NC (with opposite sign to CFS), we detected co-located clusters in most, with very strong statistical inference in the caudal pons (equivalent of 2s regression10 in Table 2) and right prefrontal WM (11 in Table 2). Clusters detected in other locations and with other NC regressions will be reported elsewhere.

We suggest that MRI correlations in NC reflect the functional consequences of normal variability in brain anatomy. In CFS we propose that the functional consequences of normal anatomical variability are distorted by impaired brainstem/midbrain signalling. Thus, in combination with impaired brainstem/midbrain signalling in CFS, normal anatomical variability could explain the correlations observed here.

Correlations in the PCC and cerebellar vermis were of interest because they mediate BP and HR in response to stress (Critchley et al., 2000; Gianaros et al., 2005; Wager et al., 2009). Such stressor response nuclei connect with nuclei in the hypothalamus, midbrain and vasomotor centre and collectively are known as the central autonomic network (CAN). Abnormal correlations with *steady state* BP and HR in some *stressor response* nuclei here may also be a consequence of compromised signalling within the brainstem/midbrain. Abnormal correlations with HR were detected in prefrontal WM tracts and are exceptions to the pattern of CAN locations detected here, although in part they connect CAN locations (Schondorf and Low, 1993). Future work that may replicate or expand upon these exploratory findings may shed more light on the mechanisms underlying these correlations.

In about a half of the clusters in Table 2, adjustment (controlling) for A&D appreciably changed cluster *P*, indicating that variance associated with A&D was present. If uncorrelated with the hemodynamic regressor variance, its removal enhanced the statistics, but if correlated, its removal weakened the statistics and A&D may have been partly causative.

4.1. Can stress explain BP and HR correlations?

We chose to measure 24 hour BP and HR in the home to minimise any effect from psychological stress. It remains possible, however, that some subjects were experiencing ambient stress levels from having a chronic illness that affected their BP and/or HR. This could naturally lead to BP or HR correlations with brain MRI in stressor-response nuclei. Similar effects should also be seen in NC (at lower levels of stress). However, for the eight 2s regressions in Table 2 the CFS and NC correlations were of *opposite* sign, which is not consistent with a stress-driven explanation for the abnormal CFS correlations. Some of the 1s CFS correlations could, however, be explained by stress modulated BP or HR changes. Clearly, it would be desirable to record levels of psychological stress and control for it, as we have done here for anxiety and depression.

4.2. Limitations

This study relied heavily on correlational analysis. Although the limitations for direction of causality apply, the conclusions presented here depend on the striking pattern of abnormal correlations being detected in brain locations largely confined to the CAN. The non-rigorous nature of ABPM in the home may have affected results. MRI signals from small nuclei within the hypothalamus, brainstem and midbrain may have been reduced by the effective spatial resolution in the final statistical analysis. Finally, support here for pathology that affects nerve signal conduction in the brainstem/midbrain relies on indirect consequential

evidence and confirmation via direct measurement of functional connectivity through/within the brainstem/midbrain is called for.

5. Conclusion

This cross-sectional study detected local abnormal correlations in CFS between brain MRI and *steady state* peripheral BP and HR. Among other regions, nuclei in the vasomotor centre, midbrain CnF, hypothalamus, cerebellar vermis and PCC were prominent. We suggest that reciprocal connectivity *between* these regulatory nuclei is impaired, which in turn affects signalling to/from peripheral effectors/sensors and culminates in the observed abnormal correlations. More research should be directed to investigating brainstem/midbrain status and function in CFS.

Acknowledgements

We thank Donald Staines for useful discussions on this work. This work was undertaken with funding from The Judith Jane Mason Foundation, the John T Reid Charitable Trusts, The Queen Elizabeth Hospital Nuclear Medicine Trust Fund and the Alison Hunter Memorial Foundation who also provided administrative assistance. These funding sources had no involvement in the design of this study. Important imaging support was provided by The Queen Elizabeth Hospital Radiology department.

References

Abbott, D., Pell, G., Pardoe, H., Jackson, G., 2009. Voxel-Based Iterative Sensitivity (VBIS): methods and a validation of intensity scaling for T2-weighted imaging of hippocampal sclerosis. NeuroImage 44, 812–819.

Barnden, L., Crouch, B., Kwiatek, R., Burnet, R., Del Fante, P., 2015. Evidence in chronic fatigue syndrome for severity-dependent upregulation of prefrontal myelination that is independent of anxiety and depression. NMR Biomed. 28 (3), 404–413. http://dx.doi.org/10.1002/nbm3261.

Barnden, L., Crouch, B., Kwiatek, R., Burnet, R., Mernone, A., Chryssidis, S., Scroop, G., Del Fante, P., 2011. A brain MRI study of chronic fatigue syndrome: evidence of brainstem dysfunction and altered homeostasis. NMR Biomed. 24 (10), 1302–1312. http://dx.doi.org/10.1002/nbm.1692.

Baroncini, M., Jissendi, P., Balland, E., Besson, P., Pruvo, J., Francke, J., Dewailly, D., Blond, S., Prevot, V., 2012. MRI atlas of the human hypothalamus. NeuroImage 59, 168–180. http://dx.doi.org/10.1016/j.neuroimage.2011.07.013.

Beacher, F., Gray, M., Mathias, C., Critchley, H., 2009. Vulnerability to simple faints is predicted by regional differences in brain anatomy. NeuroImage 47, 937–945.

Beauchet, O., Celle, S., Roche, F., Bartha, R., Montero-Odasso, M., Allali, G., Annweiler, C., 2013. Blood pressure levels and brain volume reduction: a systematic review and meta-analysis. J. Hypertens. 31, 1502–1516. http://dx.doi.org/10.1097/HJH.0b013e32836184b5.

Beaumont, A., Burton, A., Lemon, J., Bennett, B., Lloyd, A., Vollmer-Conna, U., 2012. Reduced cardiac vagal modulation impacts on cognitive performance in chronic fatigue syndrome. PLoS One 7, e49518.

Boneva, R., Decker, M., Maloney, E., Lin, J.-M., Jones, J., Helgason, H., Hein, C., Rye, D., Reeves, W., 2007. Higher heart rate and reduced heart rate variability persist during sleep in chronic fatigue syndrome: a population-based study. Auton. Neurosci. 137, 94–101.

Burnet, R., Chatterton, B., 2004. Gastric emptying is delayed in chronic fatigue syndrome. BMC Gastroenterol. 4, 32–35. http://dx.doi.org/10.1186/1471-230X-4-32.

Burton, A., Rahman, K., Kadota, Y., Lloyd, A., Vollmer-Conna, U., 2010. Reduced heart rate variability predicts poor sleep quality in a case-control study of chronic fatigue syndrome. Exp. Brain Res.

Bushberg, J., Seibert, J., Leidholdt, E., Boone, J., 2002. The essential physics of medical imaging. second ed. Lippincott, Williams and Wilkins, Philadelphia.

Carruthers, B., van de Sande, M., DeMeirleir, K., Klimas, N., Broderick, G., Mitchell, T., Staines, D., Powles, A., Speight, N., Vallings, R., Bateman, L., Baumgarten-Austrheim, B., Bell, D., Carlo-Stella, N., Chia, J., Darragh, A., Lewis, D., Jo, D., Light, A., Marshall-Gradisnik, S., Mena, I., Mikovits, J., Miwa, K., Murovska, M., Pall, M., Stevens, S., 2011. Myalgic encephalomyelitis: International Consensus Criteria. J. Intern. Med. 270, 327–338.

Cechetto, D., Shoemaker, J., 2009. Functional neuroanatomy of autonomic regulation. NeuroImage 47, 795–803.

Critchley, H., Corfield, D., Chandler, M., Mathias, C., Dolan, R., 2000. Cerebral correlates of autonomic cardiovascular arousal: a functional neuroimaging investigation in humans. J. Physiol. 523, 259–270.

Gerrity, T., Bates, J., Bell, D., Chrousos, G., Furst, G., Hedricke, T., Hurwitz, B., Kula, R., Levine, S., Moore, R., Schondorf, R., 2002. Chronic Fatigue Syndrome: what role does the autonomic nervous system play in the pathophysiology of this complex illness? Neuroimmunomodulation 10, 134–141.

Gianaros, P., Sheu, L., 2009. A review of neuroimaging studies of stressor-evoked blood pressure reactivity: emerging evidence for a brain-body pathway to coronary heart disease risk. NeuroImage 47, 922–936.

Gianaros, P., Greer, P., Ryan, C., Jennings, J., 2006. Higher blood pressure predicts lower regional grey matter volume: consequences on short-term information processing. NeuroImage 31, 754–765. http://dx.doi.org/10.1016/j.neuroimage.2006.01.003.

Gianaros, P., May, J., Siegle, G., Jennings, J., 2005. Is there a functional neural correlate of individual differences in cardiovascular reactivity? Psychosom. Med. 67, 31–39.

Hall, J., 2011. Guyton and Hall Textbook of Physiology. Saunders Elsevier, Philadelphia.

Hayasaka, S., Phan, K., Liberzon, I., Worsley, K., Nichols, T., 2004. Nonstationary cluster-size inference with random field and permutation methods. NeuroImage 22, 676–687.

He, J., Hollingsworth, K., Newton, J., Blamire, A., 2013. Cerebral vascular control is associated with skeletal muscle pH in chronic fatigue syndrome patients both at rest and during dynamic stimulation. NeuroImage Clin. 2, 168–173.

Hurwitz, B., Corvell, V., Parker, M., Laperriere, A., Klimas, N., Sfakianakis, G., Bilsker, M., 2010. Chronic fatigue syndrome: illness severity, sedentary lifestyle, blood volume and evidence of diminished cardiac function. Clin. Sci. (Lond.) 118, 125–135.

James, C., Macefield, V., Henderson, L., 2013. Real-time imaging of cortical and subcortical control of muscle sympathetic nerve activity in awake human subjects. NeuroImage 70, 59–65.

Jones, D., Hollingsworth, K., Jakovljevic, D., Fattakhova, G., Pairman, J., Blamire, A., Trenell, M., Newton, J., 2012. Loss of capacity to recover from acidosis on repeat exercise in chronic fatigue syndrome: a case–control study. Eur. J. Clin. Investig. 42, 186–194. http://dx.doi.org/10.1111/j.1365-2362.2011.02567.x.

Jones, D., Hollingsworth, K., Taylor, R., Blamire, A., Newton, J., 2010. Abnormalities in pH handling by peripheral muscle and potential regulation by the autonomic nervous system in chronic fatigue syndrome. J. Intern. Med. 267, 394–401. http://dx.doi.org/10.1111/j.1365-2796.2009.02160.x.

Lee, M., Zambreanu, L., Menon, K., Tracey, I., 2008. Identifying brain activity specifically related to the maintenance and perceptual consequence of central sensitization in humans. J. Neurosci. 28, 11642–11649.

Lewis, I., Pairman, J., Spickett, G., Newton, J., 2013. Clinical characteristics of a novel subgroup of chronic fatigue syndrome patients with postural orthostatictachycardia syndrome. J. Intern. Med. 273, 501–510.

Macefield, V., Henderson, L., 2010. Real-time imaging of the medullary circuitry involved in the generation of spontaneous muscle sympathetic nerve activity in awake subjects. Hum. Brain Mapp. 31, 539–549. http://dx.doi.org/10.1002/hbm.20885.

Maes, M., Mihaylova, I., Leunis, J.-C., 2006. Increased serum IgA and IgM against LPS of enterobacteria in chronic fatigue syndrome (CFS): indication for the involvement of gram-negative enterobacteria in the etiology of CFS and for the presence of an increased gut-intestinal permeability. J. Affect. Disord. 99, 237–240.

Meeus, M., Goubert, D., DeBacker, F., Struyf, F., Hermans, L., Coppieters, I., DeWandele, I., DaSilva, H., Calders, P., 2013. Heart rate variability in patients with fibromyalgia and patients with chronic fatigue syndrome: a systematic review. Semin. Arthritis Rheum. 43, 279–287. http://dx.doi.org/10.1016/j.semarthrit.2013.03.00.

Naidich, T., Duvernoy, H., Delman, B., Sorenson, A., Kollias, S., Haacke, E., 2009. Duvernoy's Atlas of the Brainstem and Cerebellum. High-Field MRI: Surface Anatomy, Internal Structure, Vascularisation and 3D Anatomy. SpringerWienNewYork.

Newton, J., Okonkwo, O., Sutcliffe, K., Seth, A., Shin, J., Jones, D., 2007. Symptoms of autonomic dysfunction in chronic fatigue syndrome. Q. J. Med. 100, 519–526.

Nijs, J., Ickmans, K., 2013. Postural orthostatic tachycardia syndrome as a clinically important subgroup of chronic fatigue syndrome: further evidence for central nervous system dysfunctioning. J. Intern. Med. 273, 498–500. http://dx.doi.org/10.1111/joim.12034.

Nolte, J., Angevine, J.B.J., 2000. The Human Brain in Photographs and Diagrams. second ed. Mosby, St. Louis.

Pazderka-Robinson, H., Morrison, J., Flor-Henrya, P., 2004. Electrodermal dissociation of chronic fatigue and depression: evidence for distinct physiological mechanisms. Int. J. Psychophysiol. 53, 171–182. http://dx.doi.org/10.1016/j.ijpsycho.2004.03.004.

Schondorf, R., Low, P., 1993. Idiopathic postural orthostatic tachycardia syndrome: an attenuated form of acute pandysautonomia? Neurology 43, 132–137.

Van Cauwenbergh, D., Nijs, J., Kos, D., Van Weijnen, L., Struyf, F., Meeus, M., 2014. Malfunctioning of the autonomic nervous system in patients with chronic fatigue syndrome: a systematic literature review. Eur. J. Clin. Investig. 44, 516–526.

Wager, T., Waugh, C., Lindquist, M., Noll, D., Fredrickson, B., Taylor, S., 2009. Brain mediators of cardiovascular responses to social threat, Part I: Reciprocal dorsal and ventral sub-regions of the medial prefrontal cortex and heart-rate reactivity. NeuroImage 47, 821–835.

Wyller, V., Godang, K., Morkrid, L., Saul, J., Thaulow, E., Walloe, L., 2007. Abnormal thermoregulatory responses in adolescents with chronic fatigue syndrome: relation to clinical symptoms. Pediatrics 120, e129–e137.

Zigmond, A., Snaith, R., 1983. The Hospital Anxiety and Depression Scale. Acta Psychiatr. Scand. 67, 361–370.